Biogeosciences, 14, 2183–2198, 2017
www.biogeosciences.net/14/2183/2017/
doi:10.5194/bg-14-2183-2017

Biogeosciences

Dynamics of riverine CO_2 in the Yangtze River fluvial network and their implications for carbon evasion

Lishan Ran[1], **Xi Xi Lu**[2,3], **and Shaoda Liu**[2]

[1]Department of geography, The University of Hong Kong, Pokfulam Road, Hong Kong SAR, China
[2]Department of geography, National University of Singapore, 117570, Singapore
[3]College of Environment & Resources, Inner Mongolia University, Hohhot, 010021, China

Correspondence to: Xi Xi Lu (geoluxx@nus.edu.sg)

Received: 23 November 2016 – Discussion started: 12 December 2016
Revised: 28 March 2017 – Accepted: 10 April 2017 – Published: 28 April 2017

Abstract. Understanding riverine carbon dynamics is critical for not only better estimates of various carbon fluxes but also evaluating their significance in the global carbon budget. As an important pathway of global land–ocean carbon exchange, the Yangtze River has received less attention regarding its vertical carbon evasion compared with lateral transport. Using long-term water chemistry data, we calculated CO_2 partial pressure ($p\mathrm{CO_2}$) from pH and alkalinity and examined its spatial and temporal dynamics and the impacts of environmental settings. With alkalinity ranging from 415 to $> 3400\,\mu\mathrm{eq\,L^{-1}}$, the river waters were supersaturated with dissolved CO_2, generally 2–20-fold the atmospheric equilibrium (i.e., 390 µatm). Changes in $p\mathrm{CO_2}$ were collectively controlled by carbon inputs from terrestrial ecosystems, hydrological regime, and rock weathering. High $p\mathrm{CO_2}$ values were observed spatially in catchments with abundant carbonate presence and seasonally in the wet season when recently fixed organic matter was exported into the river network. In-stream processing of organic matter facilitated CO_2 production and sustained the high $p\mathrm{CO_2}$, although the alkalinity presented an apparent dilution effect with water discharge. The decreasing $p\mathrm{CO_2}$ from the smallest headwater streams through tributaries to the mainstem channel illustrates the significance of direct terrestrial carbon inputs in controlling riverine CO_2. With a basin-wide mean $p\mathrm{CO_2}$ of 2662 ± 1240 µatm, substantial CO_2 evasion from the Yangtze River fluvial network is expected. Future research efforts are needed to quantify the amount of CO_2 evasion and assess its biogeochemical implications for watershed-scale carbon cycle. In view of the Yangtze River's relative importance in global carbon export, its CO_2 evasion would be significant for global carbon budget.

1 Introduction

Inland waters, including rivers, streams, lakes, wetland, and reservoirs, have recently been recognized as active components of the global carbon (C) cycle, transporting, storing, and processing huge amounts of terrestrially derived carbon (Aufdenkampe et al., 2011; Cole et al., 2007; Raymond et al., 2013; Richey et al., 2002; Weyhenmeyer et al., 2015; Borges et al., 2015). With a higher CO_2 partial pressure ($p\mathrm{CO_2}$) than the atmospheric equilibrium (i.e., 390 µatm), inland waters are mostly net carbon sources to the atmosphere. Published studies show that the annually degassed CO_2 from inland waters is estimated to almost entirely compensate for the total annual carbon uptake by ocean systems (Wanninkhof et al., 2013; Regnier et al., 2013). Global estimates of CO_2 evasion from rivers and streams range from 0.56 to $1.8\,\mathrm{PgC\,yr^{-1}}$ (Aufdenkampe et al., 2011; Raymond et al., 2013; Lauerwald et al., 2015). It is apparent that these results vary considerably and are associated with great uncertainties. The most recent estimate of $0.65\,\mathrm{PgC\,yr^{-1}}$ by Lauerwald et al. (2015) accounts for only 36 % of the efflux estimated by Raymond et al. (2013). While both studies have used the same hydrochemical database (GloRiCh), it should be noted that Raymond et al. (2013) used all the calculated $p\mathrm{CO_2}$ values, whereas Lauerwald et al. (2015) used only 18 % of the sampling locations. Among the numerous factors contributing to current CO_2 evasion uncertainties, a principal reason is the absence of a spatially explicit $p\mathrm{CO_2}$ data set that covers the full spectrum of the global river and stream network.

Existing global maps of CO_2 evasion from fluvial network are typically generated on the basis of incomplete spatial coverage of $p\mathrm{CO_2}$, in which Asian rivers are heavily underrepresented (e.g., Aufdenkampe et al., 2011; Battin et al., 2009; Lauerwald et al., 2015; Raymond et al., 2013). Due to a lack of direct in situ measurements, simplified extrapolation is normally used to predict $p\mathrm{CO_2}$ in and CO_2 evasion from Asian river systems. Consequently, the estimation accuracy is problematic and even erroneous. For example, for the Yellow River in East Asia, while the calculated $p\mathrm{CO_2}$ from river water chemistry is 2800 µatm (Ran et al., 2015a), the modeled $p\mathrm{CO_2}$ by Lauerwald et al. (2015) is 30 % lower (i.e., < 2000 µatm). A much lower estimate of < 700 µatm can be derived from the $p\mathrm{CO_2}$ map produced in Raymond et al. (2013). Such great discrepancies are largely because riverine $p\mathrm{CO_2}$ is highly site-specific and affected by a wide range of environmental factors (e.g., Abril et al., 2015; Teodoru et al., 2015). Asian rivers are significant contributors to global carbon flux as a result of high soil erosion and particulate organic carbon export, accounting for 40 % of the global carbon flux from land to sea (Schlünz and Schneider, 2000; Hope et al., 1994). Estimating the amount of CO_2 degassed from Asian rivers is critical for global CO_2 evasion assessments. Recent work in the Mekong and Yellow rivers has demonstrated high $p\mathrm{CO_2}$ and CO_2 effluxes (Alin et al., 2011; Ran et al., 2015b), further highlighting the necessity of incorporating the currently underrepresented Asian rivers into global carbon budget assessments.

As an important carbon contributor to the western Pacific Ocean, the Yangtze River has received widespread attention in fluvial carbon export at various spatial and temporal scales. Studies of flux estimates of different carbon species date back to the early 1980s (Cauwet and Mackenzie, 1993; Gan et al., 1983; Milliman et al., 1984; Wang et al., 2012; Zhang et al., 2014; Ittekkot, 1988). Intensive observations covering seasonal variability show that the Yangtze River transports approximately 20 Mt of C per year into the oceans (Wu et al., 2007; Bao et al., 2015). Contrary to the long history of lateral export measurements, however, few studies have examined the vertical carbon exchange between the river system and the atmosphere (Li et al., 2012; Zhao et al., 2013; Chen et al., 2008). This is by nature largely due to the differences in sampling strategy. Unlike the lateral export that only involves measurements on the mainstem or at specific sites near the river mouth, quantifying basin-wide CO_2 evasion requires a spatially explicit $p\mathrm{CO_2}$ data set encompassing the entire fluvial network. Any attempts of using limited local measurements to up-scale to the watershed scale are challenging and subject to large uncertainties. This has impacted the understanding of the riverine carbon cycle within the Yangtze River watershed as well as its links to the atmosphere and ocean systems.

By using long-term water chemistry data measured in the Yangtze River watershed, we calculated the riverine $p\mathrm{CO_2}$ from pH and alkalinity. In combination with hydrologic and lithologic information, the objectives of this study were to (1) investigate the spatial and temporal patterns of $p\mathrm{CO_2}$ under "natural" processes before significant human perturbations, mainly dam impoundment and land-use change since the 1990s and (2) to explore the couplings between $p\mathrm{CO_2}$ and environmental settings by investigating environmental and geomorphologic controls. Based on the obtained $p\mathrm{CO_2}$, we further evaluated its biogeochemical implications for CO_2 evasion. In view of the Yangtze River's role in global fluvial export of water, sediment, and carbon (Syvitski et al., 2005; Wang et al., 2012), its contribution to the global CO_2 evasion from river systems is likely significant. This $p\mathrm{CO_2}$ database is thus helpful to examine the spatial distribution of global riverine $p\mathrm{CO_2}$ and to refine estimates of global CO_2 evasion.

2 Material and methods

2.1 The Yangtze River basin

With a length of 6380 km, the Yangtze River is the longest river in China and the third longest in the world. The river originates on the Tibetan Plateau and flows eastward through the Sichuan Basin and the Middle–Lower Reach Plains, before emptying into the East China Sea (Fig. 1a). Its drainage area is 1.81 million km^2. The Yangtze River basin is mainly overlain by sedimentary rocks that are composed of marine carbonates, evaporites, and continental deposits. Carbonate sedimentary rocks are widely distributed within the watershed and are particularly abundant in the Wujiang, Yuanjiang, and Hanjiang tributary catchments (Fig. 1b). Siliciclastic sedimentary rocks are also widely present in the basin while metamorphic rocks are mainly scattered in the middle–lower reach (Fig. 1b). The Yangtze River is joined by a number of large tributaries, including the Yalongjiang, Daduhe, Minjiang, Jialingjiang, Wujiang, Yuanjiang, Xiangjiang, Hanjiang, and Ganjiang rivers (Fig. 1a).

Except the headwater region characterized by high elevation and cold climate (annual mean temperature < 4 °C), the remaining watershed is affected by subtropical monsoons with the annual mean temperature in the middle–lower reach varying from 16 to 18 °C (Chen et al., 2002). Rainfall is the major source of water discharge, whereas snowfall supply is only significant in the ice-covered upstream mountainous areas. With a mean precipitation of 1100 $\mathrm{mm\,yr^{-1}}$, the precipitation is spatially highly variable, decreasing from 1644 $\mathrm{mm\,yr^{-1}}$ in the lower reach, to 1396 $\mathrm{mm\,yr^{-1}}$ in the middle reach, and 435 $\mathrm{mm\,yr^{-1}}$ in the upper reach (Chetelat et al., 2008). Approximately 60 % of the annual precipitation falls during the wet season from June to September. Affected by summer monsoons, the wet season generally occurs ear-

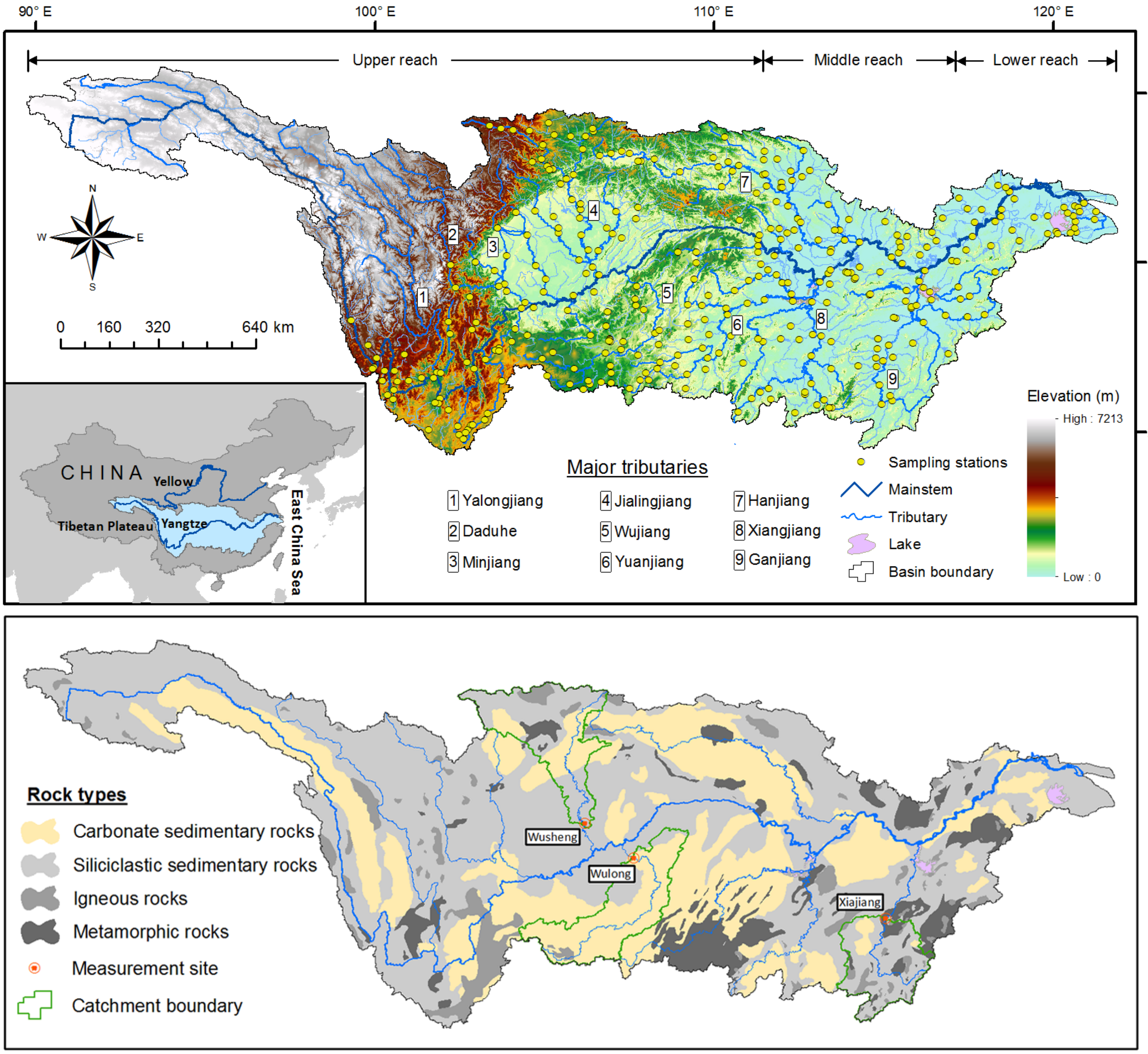

Figure 1. Maps of the Yangtze River basin showing sampling stations (top) and rock compositions (bottom). Rock information is modified from Chen et al. (2002) and Chetelat et al. (2008).

lier in the middle and lower reaches than in the inland upper reach. Water discharge from the upper to the lower reach presents a strong seasonal variability (Fig. 2). Monthly peak discharge occurs in July and can be 5–7 times greater than the lowest discharge in the dry season (October to May). The mean discharge at Datong station is 28 200 $m^3\,s^{-1}$ (see its location in Fig. 3b), and consequently the Yangtze River annually discharges 889 km^3 of water into the ocean (Yang et al., 2002).

2.2 Water chemistry data

Concentrations of alkalinity, major ions, and dissolved silica measured at 359 stations in the Yangtze River watershed (Fig. 1a) during the period 1960s–1985 were retrieved from the Hydrological Yearbooks, which were yearly produced by the Yangtze River Conservancy Commission (YRCC) for internal use. Concomitant environmental variables measured at each sampling event, including pH, water temperature, and discharge, were also extracted from the yearbooks. The water samples for pH and temperature measurement were taken in the same period as these for ion analysis. The sampling frequency ranged from 1 to 14 times per month depending

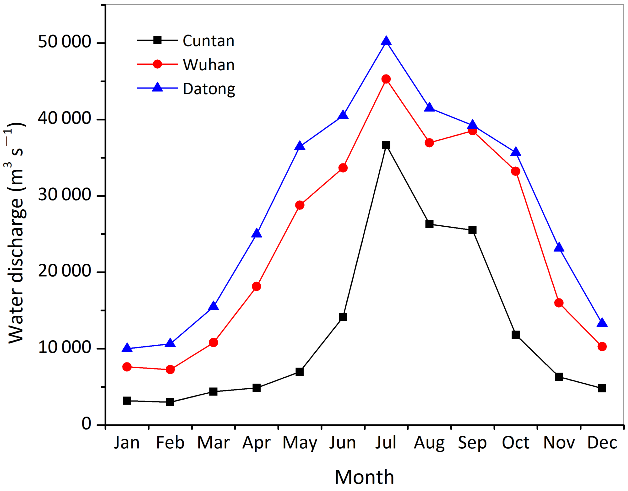

Figure 2. Monthly variations in water discharge of the Yangtze River at Cuntan (upper reach), Wuhan (middle reach), and Datong stations (lower reach).

on flow conditions. While sampling at some stations during 1966–1975 was less frequent, ∼ 80 % of the 359 stations have been continuously sampled for at least 10 years, starting from the early 1970s. To avoid severe river pollution by human activity, only the samples collected prior to 1985 were used. In addition, samples with a pH lower than 6.5 were manually discarded (498 measurements; predominantly in the lower reach) because the calculated pCO_2 would be greatly biased due to contributions of noncarbonated alkalinity such as organic acid anions (Abril et al., 2015; Hunt et al., 2011). Because reservoir trapping and increased water residence time can remarkably alter the physical and biogeochemical properties of running water (Kemenes et al., 2011; Barros et al., 2011), the stations located inside or shortly below reservoirs were also intentionally removed. Given the tidal influences, mainstem stations downstream of Datong, 626 km inland from the coast, were also excluded, as were the stations in the delta region that were affected either by tides or by intersections with other rivers via artificial canals. Based on these selection criteria, 339 stations, including 13 mainstem stations and 326 tributary stations, were retained and 47 809 water chemistry measurements in total were compiled. The discarded samples owing to $\text{pH} < 6.5$ accounted for approximately 1 % of the considered measurements. No sampling station was excluded solely because it had $\text{pH} < 6.5$ samples only.

Chemical analyses of water samples were performed under the authority of YRCC following the standard procedures and protocols described by Alekin et al. (1973) and the American Public Health Association (1985). While pH and temperature were measured in the field, the alkalinity was determined by acid titration. Detailed sampling and analysis procedures were presented in Chen et al. (2002). One important issue regarding historical records is data reliability. No assessment reports on quality assurance and quality control are available in the hydrological yearbooks. An effective evaluation approach is to compare the hydrochemical differences for samples collected at the same station but by different agencies. The Wuhan station on the Yangtze mainstem has also been monitored under the United Nations GEMS/Water Programme since 1980 (only yearly means available at http://www.unep.org/gemswater). The pH value from the yearbooks agreed well with that measured by the GEMS/Water Programme with < 1.8 % differences, while the alkalinity discrepancy between the two data sets is larger (Table 1). The yearbooks report a slightly higher alkalinity than the GEMS/Water Programme results by 7.6–13.9 %, indicating that the yearbook reports are reliable for pCO_2 calculation. High data quality of the yearbook reports can also be validated from comparison of major dissolved elements measured by the two agencies at Wuhan station (see Chen et al., 2002).

2.3 Calculation of pCO_2

The conventional method of calculating pCO_2 from pH and alkalinity was used. With ∼ 90 % of the pH values ranging from 7.1 to 8.3 suggestive of natural process for the Yangtze River, bicarbonates were assumed equivalent to alkalinity (Amiotte-Suchet et al., 2003), accounting for 96 % of the total alkalinity. As a result of low dissolved organic carbon (i.e., < 250 µM; Liu et al., 2016), impact of organic acids on alkalinity is predicted to be small. The pCO_2 was then calculated using the program CO2SYS (Lewis and Wallace, 1998). However, using this method would produce biased extreme values that are unrealistic in natural river systems (Hunt et al., 2011; Weyhenmeyer et al., 2015). We thus reported median values per sampling station instead of means to avoid the impact of erroneous extreme results. The results were summarized in the Supplement (Table S1).

3 Results

3.1 Spatiotemporal variability in alkalinity and pCO_2

Except the excluded measurements, pH in the Yangtze River waters varied from 6.5 to 9.2 with 96 % of the pH measurements ranging from 7.3 to 8.3 (Table 2). Higher pH values (i.e., > 7.8) were spatially measured in the headwater streams and the Hanjiang catchments (see Fig. 1a for location). In comparison, the tributaries in the southern part of the watershed exhibited relatively low pH values. For the mainstem channel (Table 2), the median pH showed a significant downstream decrease from 8.29 to 7.55 ($r^2 = 0.77$; $p < 0.001$). The alkalinity varied from 415 to > 3400 $\mu eq\,L^{-1}$ (Fig. 3a). Higher alkalinity (i.e., > 2500 $\mu eq\,L^{-1}$) was observed in the upper reach and the upper part of the middle reach (Fig. 3a), in particular the carbonate-rich tributary

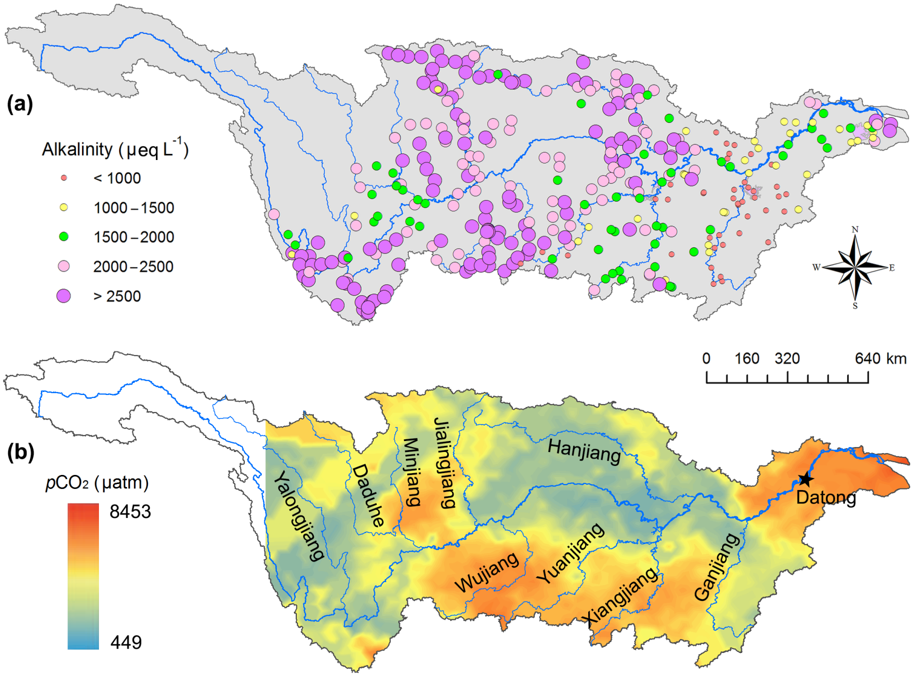

Figure 3. Spatial distribution of alkalinity **(a)** and $p\mathrm{CO_2}$ **(b)** in the Yangtze River basin. The headwater region in panel **(b)** was not interpolated because of insufficient stations.

Table 1. Comparison of alkalinity (μeq L^{-1}) and pH at Wuhan station between the GEMS/Water Programme results and the hydrological yearbooks, expressed as mean ± standard error.

Item	1980	1981	1982	1983	1984	1984
			GEMS/Water Programme			
Alkalinity	2050 ± 286	2004 ± 188	2000 ± 232	1838 ± 252	2200 ± 247	1992 ± 219
pH	7.83 ± 0.16	7.73 ± 0.24	8.04 ± 0.09	8.06 ± 0.05	8.00 ± 0.09	7.88 ± 0.06
			Hydrological yearbooks			
Alkalinity	2310 ± 314	2187 ± 236	2274 ± 268	2033 ± 304	2383 ± 277	2306 ± 238
pH	7.93 ± 0.09	7.87 ± 09	8.01 ± 0.09	7.94 ± 0.08	7.93 ± 0.10	7.98 ± 0.08

catchments (e.g., the Jialingjiang, Wujiang, and Hanjiang rivers). In contrast, the lower part of the middle reach (mainly the Ganjiang River) and the lower reach showed a lower alkalinity of < 2000 μeq L^{-1}. The average alkalinity over the whole watershed was 2210 ± 1023 μeq L^{-1}.

The calculated $p\mathrm{CO_2}$ varied by a magnitude of 2 with the highest $p\mathrm{CO_2}$ being 24 432 μatm. At 95 % of the stations, the $p\mathrm{CO_2}$ was higher than 1000 μatm, generally 2–20-fold the atmospheric $p\mathrm{CO_2}$. Only one station in the upper reach showed a median $p\mathrm{CO_2}$ lower than the atmosphere. In the mainstem, the $p\mathrm{CO_2}$ increased from ∼ 700 μatm at the uppermost station to 3800 μatm at Nanjing near the river mouth (Table 2). Averaged over all stations, the basin-wide $p\mathrm{CO_2}$ was 2662 ± 1240 μatm. To better illustrate its spatial variability, we modeled the $p\mathrm{CO_2}$ for the whole stream network using the Kriging interpolation method in ArcGIS 10.1 (Esri, USA) with the assumption that the station-based $p\mathrm{CO_2}$ was representative of the surrounding streams. Similar to alkalinity, the $p\mathrm{CO_2}$ presented significant spatial variations (Fig. 3b). The Yangtze mainstem near the headwater region and the Yalongjiang catchment showed the lowest $p\mathrm{CO_2}$, generally < 1000 μatm. In comparison, the carbonate-rich tributaries in the southern part of the watershed had high $p\mathrm{CO_2}$ values. With an areal coverage of 83 % by carbonate sedimentary rocks, the Wujiang catchment presented the highest median $p\mathrm{CO_2}$ than other tributaries, averaging 3550 ± 1356 μatm. In the lower reach, the$p\mathrm{CO_2}$ was 3988 ± 1244 μatm on average, which is inconsistent with its relatively low alkalinity of < 2000 μeq L^{-1} (Fig. 3a). It is worth noting that the $p\mathrm{CO_2}$ in Hanjiang catchment was lower than expected, given its high

Table 2. Riverine pH, alkalinity, and pCO$_2$ in the Yangtze River basin (median ± standard deviation)[a].

River/tributary	Station	pH	Alkalinity µeq L^{-1}	pCO$_2$ µatm
Mainstem	Benzilan	8.29 ± 0.11	2352 ± 435	681 ± 156
	Shigu	8.18 ± 0.48	2544 ± 438	846 ± 262
	Jingjiangjie	8.11 ± 0.12	2905 ± 362	916 ± 202
	Dukou	8.22 ± 0.12	2399 ± 429	826 ± 197
	Longjie	8.23 ± 0.17	2185 ± 396	786 ± 226
	Huatan	8.17 ± 0.15	2237 ± 418	882 ± 287
	Pingshan	8.13 ± 0.10	2215 ± 407	1001 ± 235
	Zhutuo	7.88 ± 0.19	2299 ± 349	2405 ± 781
	Cuntan	8.08 ± 0.11	2173 ± 311	1087 ± 319
	Yichang	7.95 ± 0.15	2343 ± 300	1653 ± 469
	Luoshan	7.76 ± 0.11	2280 ± 248	2380 ± 691
	Wuhan	7.93 ± 0.11	2060 ± 263	1521 ± 497
	Datong	7.84 ± 0.14	1919 ± 312	1711 ± 806
	Nanjing[b]	7.56 ± 0.16	2339 ± 339	3796 ± 1623
	Nanjing[c]	7.54 ± 0.18	2296 ± 357	3793 ± 2186
Major tributaries[d]				
Yalongjiang	Xiaodeshi	8.02 ± 0.22	2576 ± 465	1567 ± 715
Daduhe	Fuluzhen	7.66 ± 0.23	1909 ± 289	2577 ± 1620
Minjiang	Gaochang	8.02 ± 0.15	1816 ± 327	1020 ± 525
Tuojiang	Lijiawan	8.01 ± 0.11	2705 ± 507	1504 ± 572
Jialingjiang	Beibei	8.11 ± 0.14	2289 ± 509	1196 ± 244
Wujiang	Wulong	8.01 ± 0.14	2420 ± 279	1361 ± 508
Yuanjiang	Taoyuan	7.61 ± 0.25	1822 ± 480	2801 ± 2144
Xiangjiang	Xiangtan	7.76 ± 0.44	1739 ± 331	2349 ± 2521
Hanjiang	Xiaoshicun	7.93 ± 0.13	2262 ± 480	1715 ± 536
Ganjiang	Waizhou	7.44 ± 0.44	880 ± 236	2205 ± 2048
Yangtze Basin[e]	1st percentile	7.03	556	788
	10th percentile	7.35	842	1236
	50th percentile	7.71	2237	2455
	90th percentile	8.05	3305	4344
	99th percentile	8.28	4437	6163

[a] Station-based pCO$_2$ is summarized in Table S1; [b] affected by high tides; [c] affected by low tides; [d] median values of the data for the lowermost station on the mainstem of the specific tributary; [e] statistics based on the measurements at the 339 stations used.

alkalinity (> 2500 µeq L^{-1}). Differences in pH in these catchments are likely a principal cause of these inconsistencies.

In addition, the pCO$_2$ also showed strong temporal variability. Figure 4 presents an example of pCO$_2$ changes at Datong station on the mainstem channel. Despite considerable interannual variations that could change by a factor of 5, the annual pCO$_2$ declined steadily during the > 20-year-long sampling period ($r^2 = 0.18$; $p < 0.05$) (Fig. 4a). This trend is pronounced even if the anomalously high values in the late 1960s are excluded. Indeed, more than half of the evaluated stations, mainly in the middle–lower reach, showed a significant decreasing trend at the 95 % confidence level. In contrast, gradual increases were observed at some tributary stations in the upper reaches. Seasonally, the pCO$_2$ in the wet season was on average 30 % higher than that in the dry season (Fig. 4b), and greater fluctuation ranges could be observed in wet seasons.

3.2 Correlations with hydro-geochemical variables

Figure 5 presents two representative examples showing responses of alkalinity and pCO$_2$ to hydrological regimes. Changes in alkalinity at both stations reflected a clear dilution effect. High alkalinity concentrations were measured in low-flow periods when groundwater was the major contributor to runoff (Fig. 5a and c). Checking all stations indicated that the alkalinity at 98 % of the stations decreased exponentially with increasing water discharge after the onset of the wet season. In contrast, the pCO$_2$ presented diverse relationships with water changes (Fig. 5b and d). There was no discernible dependence of pCO$_2$ on flow in the mainstem, while

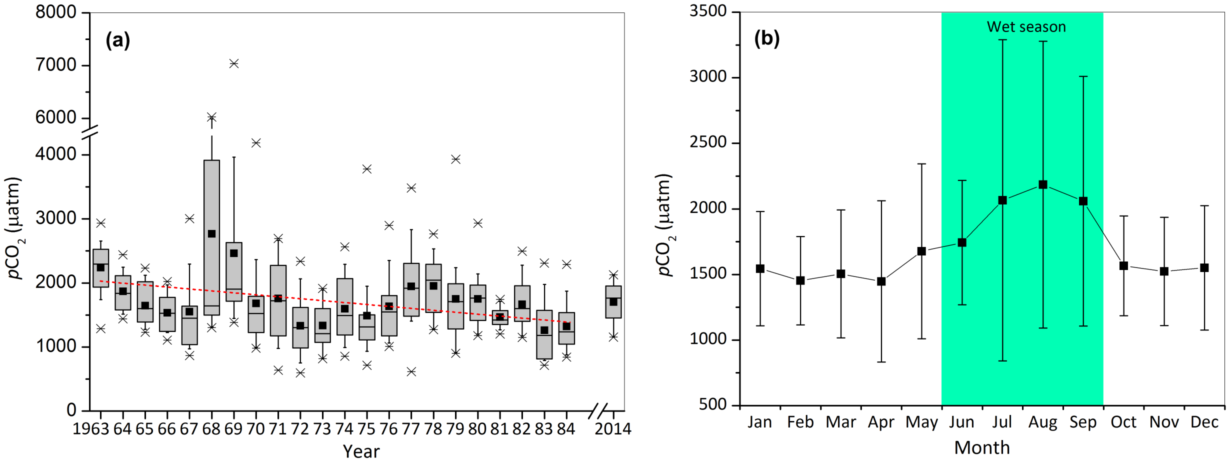

Figure 4. Temporal variations in $p CO_2$ at Datong station. **(a)** Box-and-whisker plots show significant interannual changes; **(b)** seasonal variations. The dash line in panel **(a)** represents linear regression, and the values for 2014 are derived from Liu et al. (2016). Error bars denote standard deviation.

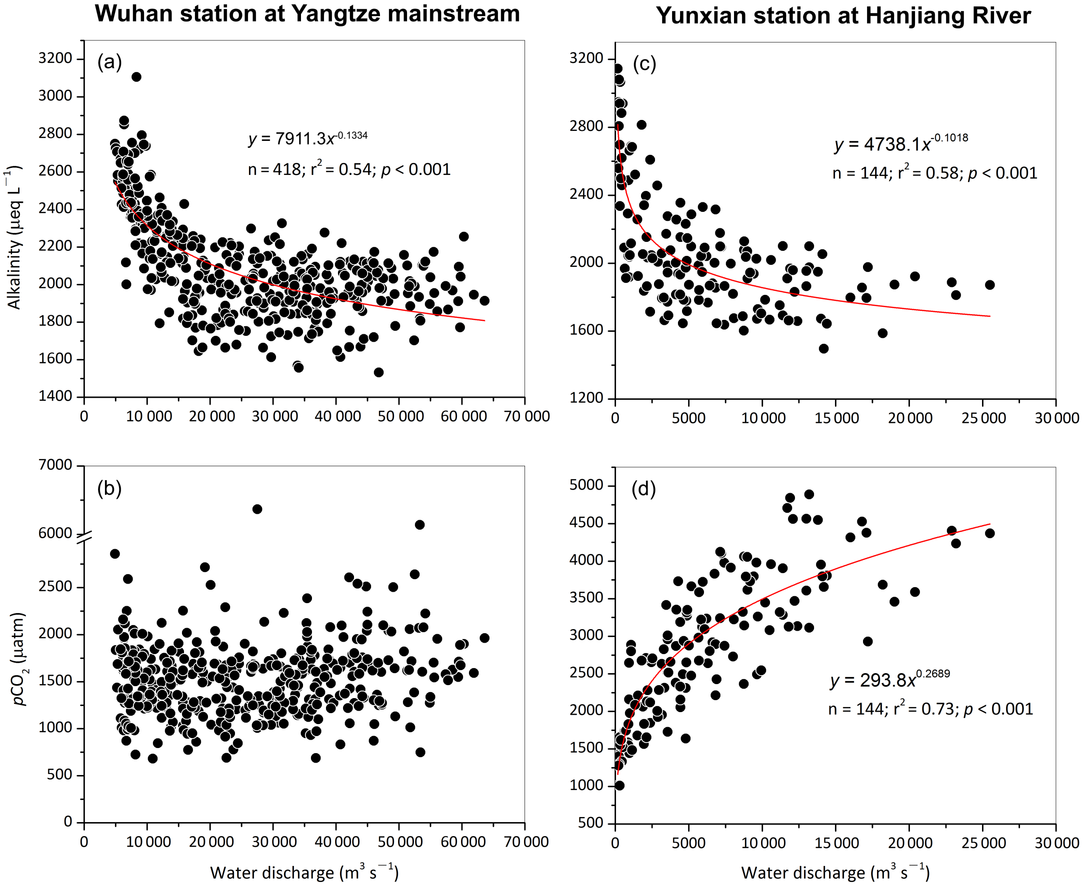

Figure 5. Correlations between water discharge and instantaneous alkalinity and $p CO_2$: the mainstem at Wuhan station **(a, b)** and the Hanjiang River at Yunxian station **(c, d)**.

Table 3. Hydro-geochemical features of the Wujiang (Wulong station), Jialingjiang (Wusheng station), and Ganjiang (Xiajiang station) catchments.

Control station	Control area km^2	Water discharge m^3 s^{-1}	pH	Alkalinity µeq L^{-1}	pCO_2 µatm	Ca^{2+} µmol L^{-1}	SiO_2 µmol L^{-1}	Sedimentary rock types (% of area)		
								Carbonate	Siliciclastic	Igneous + metamorphic
Wulong	80 536	1570	7.72 ± 0.14	3021 ± 527	3537 ± 1247	1145 ± 278	59 ± 31	82.9	14.8	2.3
Wusheng	80 550	793	7.80 ± 0.21	2484 ± 948	2671 ± 490	1005 ± 170	94 ± 30	30.4	55.3	14.3
Xiajiang	62 387	1644	7.34 ± 0.08	953 ± 266	2642 ± 626	242 ± 91	105 ± 18	9.1	64.7	26.2

a positive correlation was widely observed in small tributaries. Although only two stations were plotted here, these diverse responses of alkalinity and pCO_2 to flow changes were widespread within the watershed, in particular for pCO_2 between mainstem and small tributaries.

In order to elucidate the impacts of rock weathering on pCO_2, we selected three typical tributary catchments with differing rock compositions (Table 3). The Wujiang catchment is mainly underlain by carbonate sedimentary rocks (83 %) and the Ganjiang catchment by siliciclastic sedimentary rocks (65 %), whereas the Jialingjiang catchment lies in the middle regarding the areal coverage of the two rocks (Table 3 and Fig. 1b). As the most typical weathering products of carbonate and siliciclastic sedimentary rocks, we plotted Ca^{2+} and dissolved silica (expressed as SiO_2) against pCO_2, respectively (Fig. 6). For the three catchments with contrasting rock compositions, the pCO_2 showed different responses to Ca^{2+} and SiO_2. In Wujiang catchment, the log-transformed pCO_2 (i.e., $\lg(pCO_2)$) presented a significant negative correlation with Ca^{2+} concentration ($p < 0.001$) (Fig. 6). This negative correlation became less apparent with decreasing carbonate coverage in Jialingjiang and Ganjiang catchments. In contrast, while the $\lg(pCO_2)$ exhibited a positive correlation with SiO_2 in Jialingjiang and Ganjiang catchments characterized by high coverage of siliciclastic sedimentary rocks, no clear relation between $\lg(pCO_2)$ and SiO_2 was detected in Wujiang catchment (Fig. 6). However, when plotting pCO_2 against Ca^{2+} and SiO_2 for the entire Yangtze River watershed, there was no discernable relationship between pCO_2 and both variables (Fig. S1 in the Supplement).

4 Discussion

4.1 Uncertainty analysis of pCO_2

As an important parameter for CO_2 evasion estimation, an accurate riverine pCO_2 is essential to quantify CO_2 evasion and explore its biogeochemical implications for carbon cycle at different scales. Compared with direct measurement by means of membrane equilibration or headspace technique, the conventional pCO_2 calculation from alkalinity has been criticized for causing biases (Long et al., 2015; Hunt et al., 2011). Huge overestimations (i.e., > 100 %) have been reported in rivers with organic-rich and acidic waters due to combined effects of high organic acids and low buffering capacity of carbonate systems at low pH (Abril et al., 2015). Unfortunately, there was no organic carbon information in the yearbooks, and measurements of dissolved organic carbon (DOC) in the Yangtze River started in the early 1980s. Its DOC ranging from 130 to 180 µM was relatively low compared with other major world rivers (Bao et al., 2015; Wang et al., 2012). Our recent sampling also shows that the mean DOC is 160 µM for the mainstem and 200 µM for major tributaries (Liu et al., 2016). Given the neutral to basic pH range and the alkalinity variations, we believe the impact of organic acids is minimal, although a slight overestimation may have occurred as suggested by Abril et al. (2015). Our recent pCO_2 measurements in the mainstem and major tributaries using a membrane contactor (Qubit DCO_2 System, Qubit Biology Inc., Canada) also indicate that the calculated pCO_2 results are consistent with the measured values with only ∼ 8 % differences (Liu et al., 2016).

Furthermore, this pCO_2 calculation method is sensitive to pH changes. High accuracy of pH measurements is critical to reduce the associated uncertainty. Similar to other water chemistry records (i.e., Butman and Raymond, 2011; Lauerwald et al., 2013; Weyhenmeyer et al., 2015), the retrieved pH was reported with a precision of one decimal place. If the uncertainties in pH measurement accuracy are assumed to 0.1 pH units, the calculated pCO_2 would be underestimated by 26 % or overestimated by 21 %. To minimize human-induced disturbances in the chemical equilibrium of natural waters, we excluded the samples with pH < 6.5 and treated them as being significantly polluted. This arbitrary exclusion may have generated biased estimates of pCO_2 for the whole river network in general and some natural rivers characteristic of low pH in particular (Wallin et al., 2014). Considering the higher alkalinity than the GEMS/Water Programme results, the propagated uncertainty ranges from 14 % (underestimation) to 27 % (overestimation). As the middle–lower reach of the Yangtze River watershed is one of China's largest industrial and agricultural bases, the impact of human activities within the watershed, including sewage inputs and use of chemical fertilizers, may have altered its chemical compositions and pH. In view of the small number of dis-

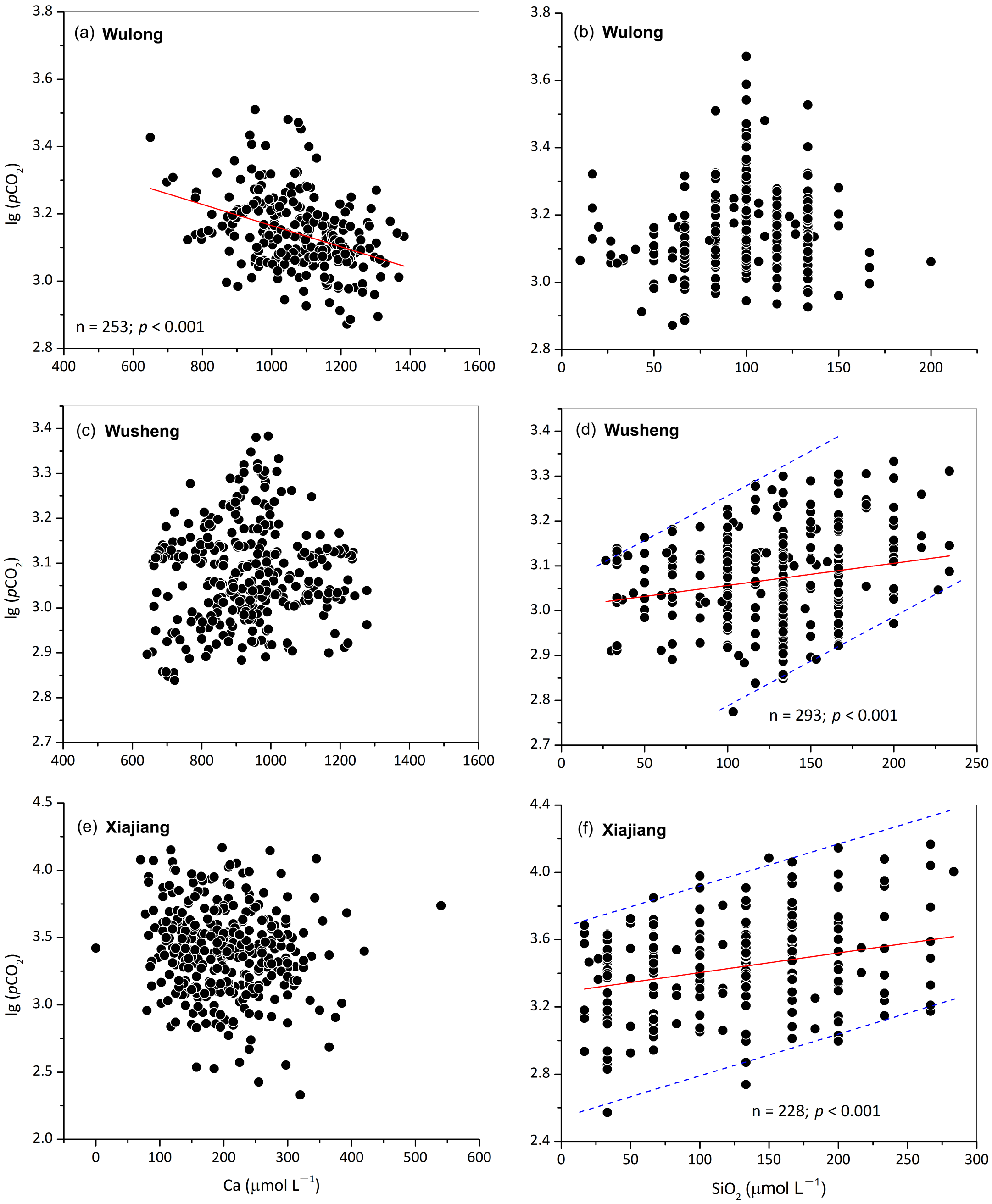

Figure 6. Responses of $p\text{CO}_2$ to rock weathering products in three typical catchments with distinct rock compositions: **(a, b)** Wujiang River (Wulong station), **(c, d)** Jialingjiang River (Wusheng station), and **(e, f)** Ganjiang River (Xiajiang station). The solid lines represent linear regression.

carded measurements (1 % of the total) and the high buffering capacity of carbonate alkalinity and low DOC contents, the calculated $p\text{CO}_2$ is reasonable and can be used for further CO_2 evasion estimation.

4.2 Environmental impacts on alkalinity and $p\text{CO}_2$

Export of alkalinity in river systems was affected by hydrological regime with a clear dilution effect (Fig. 5). The average alkalinity was 35 % lower in the wet season than in the dry season. In both the mainstem and the tributaries, the higher alkalinity during low-flow periods in dry seasons (Fig. 5a and c) illustrated the contribution of groundwater recharge in providing abundant alkalinity. With widespread carbonate presence, groundwater in the Yangtze River watershed was rich in dissolved inorganic carbon (DIC). Recent studies show that the alkalinity of typical karst groundwater in the watershed is in the range of 3300–4200 $\mu eq\,L^{-1}$ (X.-D. Li et al., 2010; S.-L. Li et al., 2010). With reduced relative contribution of groundwater in the wet season, the high alkalinity was diluted by local rain events that carried lower DIC contents. Spatially, the dilution effect was more pronounced in the upper reach than the middle–lower reach. This may have revealed the response of alkalinity production to land cover. Catchments with a higher forest cover normally exhibit a stronger dilution effect than cropland catchments (Raymond and Cole, 2003). While cropland was the major land-use type in the middle–lower reach accounting for 53.5 % of the total catchment area, forest cover in the upper Yangtze River watershed was much higher (37.3 %) than the middle–lower reach (30.4 %; data are from the Data Center for Resources and Environmental Sciences for the 1980s).

Riverine dissolved CO_2 originates primarily from terrestrial ecosystem respiration, groundwater input, and in-stream processing of land-derived organic matter (Wallin et al., 2013; Lynch et al., 2010). Different from alkalinity showing a clear dilution effect, the stable $p\mathrm{CO_2}$ in the Yangtze mainstem likely reflected the impact of different biogeochemical processes (Fig. 5b). Compared to the dry season in which the $p\mathrm{CO_2}$ was mainly controlled by DIC inputs from groundwater, the elevated $p\mathrm{CO_2}$ in the wet season suggested the influence of organic carbon transport and decomposition. Owing to strong erosion and leaching of recently fixed organic matter, its organic carbon content in the wet season is significantly higher and the age much younger (Wang et al., 2012; Zhang et al., 2014). Rapid mineralization of the labile fraction of organic carbon can increase the $p\mathrm{CO_2}$. A recent study indicates that, while ~ 60 % of the recently fixed carbon entering the Yangtze River in wet seasons can be quickly degraded, the degradation ratio is only 31 % in dry seasons (Wang et al., 2012). On the other hand, the increasing $p\mathrm{CO_2}$ with flow in tributaries indicated enhanced supply of fresh dissolved CO_2 during high-flow periods (Fig. 5d). For tributaries with more homogeneous catchment settings, decomposition of soil organic matter can provide abundant dissolved CO_2 (Liu et al., 2016; Li et al., 2012), generating a positive $p\mathrm{CO_2}$ response to water discharge. Presence of wetlands and floodplains also affects river biogeochemistry (Teodoru et al., 2015). Affected by dam impoundment, the catchment upstream of Yunxian station is characteristic of widespread wetlands and floodplains. Consequently, the enhanced connectivity between river and wetlands/floodplains along the aquatic continuum, especially during wet seasons, have maintained its high $p\mathrm{CO_2}$ levels (Abril et al., 2014). For $p\mathrm{CO_2}$ in the mainstem (Fig. 5b), it is likely because the increased dissolved CO_2 inputs by soil organic matter decomposition from one region has been counteracted by low-$p\mathrm{CO_2}$ waters derived from other regions. This is highly possible given its heterogeneous catchment settings in terms of vegetation cover, soil type, and rainfall intensity. Furthermore, the large catchment implies a long travel time of land-derived organic carbon during fluvial delivery (3–5 months). Coupled with limited floodplains along the mainstem channel (see discussion below), direct inputs of CO_2 from soil respiration would be relatively low whereas strong CO_2 evasion in lower-order turbulent tributaries might have already exhausted dissolved CO_2. Therefore, its $p\mathrm{CO_2}$ dynamics appeared to be independent of hydrograph.

The spatial distribution of alkalinity overlapped well with the outcrops of carbonate sedimentary rocks (Figs. 1b and 3a), with ~ 60 % of the high alkalinity concentrations measured in carbonate catchments. Using Ca^{2+} as a proxy of rock weathering, the strong correlation between Ca^{2+} and alkalinity suggested the dominant role of weathering in controlling alkalinity and DIC export (Fig. 7). This is consistent with the significant impact of weathering on alkalinity as observed in other rivers (Raymond and Cole, 2003; Humborg et al., 2010). Particularly, given the higher susceptibility of carbonates to weathering than silicates (Goudie and Viles, 2012), the abundant carbonate presence in Wujiang catchment helped to sustain its high alkalinity and$p\mathrm{CO_2}$ (Table 3). However, the negative correlation in Fig. 6a is contradictory to the common belief that carbonate dissolution will likely cause an elevated $p\mathrm{CO_2}$ (Marcé et al., 2015; Teodoru et al., 2015). Given the significant correlation between Ca^{2+} and alkalinity, the decreasing $p\mathrm{CO_2}$ with increasing Ca^{2+} is probably due to pH variability that may have offset the impact of weathering-induced DIC inputs in controlling $p\mathrm{CO_2}$ (Fig. S2). A slight pH increase would result in a reduced $p\mathrm{CO_2}$ as this calculation method is sensitive to pH fluctuations (Laruelle et al., 2013).

The positive correlation between $p\mathrm{CO_2}$ and SiO_2 in Jialingjiang and Ganjiang catchments demonstrated the impact of DIC export by silicate weathering. Despite the high silicate weathering rate in Ganjiang catchment, its alkalinity represented only one-third of that in the other two catchments (Table 3). Apparently, its high $p\mathrm{CO_2}$ of 2642 ± 626 µatm was primarily the result of its low pH (~ 6 % lower). Overall, the catchments with more carbonate presence presented higher $p\mathrm{CO_2}$ values (Figs. 1 and 3b). Because weathering products are typical for groundwater, this also suggests that riverine $p\mathrm{CO_2}$ has a strong groundwater signature. Different from the positive response of $p\mathrm{CO_2}$ to discharge at Yunxian station reflecting the importance of connectivity between river and wetlands/floodplains (Fig. 5d), the decreasing $p\mathrm{CO_2}$ at Xiajiang station with discharge is indicative of the impact of groundwater input on riverine carbon dynamics (Figs. S3a and 6f). Particularly, in dry seasons with groundwater dominating the runoff (Fig. S3b), SiO_2 can explain ~ 25 % of the $p\mathrm{CO_2}$ variability in sub-catchments covered mainly with siliciclastic sediment rocks, comparable to the results by Humborg et al. (2010) in Sweden. The indiscernible $p\mathrm{CO_2}$–Ca^{2+} and $p\mathrm{CO_2}$–SiO_2 relationship for the entire watershed may be

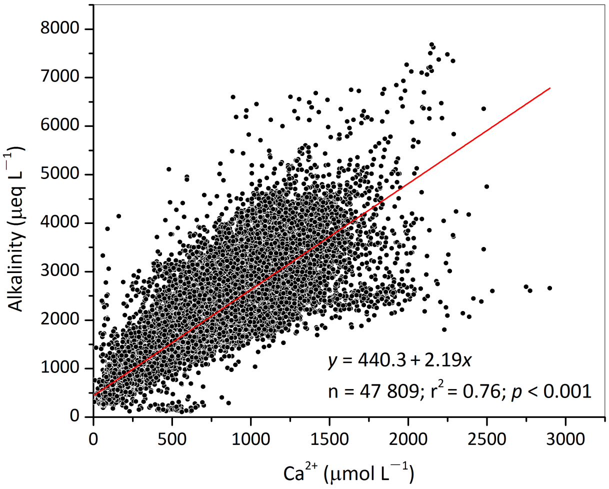

Figure 7. Strong correlation between chemical weathering, using Ca^{2+} as a proxy, and alkalinity.

attributed to the spatial heterogeneity in lithology that has obscured the signature (Fig. S1). While both positive and negative relationships existed in sub-catchments with predominant carbonate or siliciclastic sediment rocks (Fig. 6), these relationships may have counteracted each other when all data points were plotted together.

Because $p\mathrm{CO_2}$ was calculated from alkalinity, its spatial variability reflected largely the export of the latter. The inconsistencies between $p\mathrm{CO_2}$ and alkalinity in Hanjiang catchment were likely caused by dam operation (Fig. 3). By altering the physical and biogeochemical properties of flowing water, dam trapping could cause a greatly declined $p\mathrm{CO_2}$ as a result of photosynthetic CO_2 fixation and increased pH (Ran et al., 2015a). The Danjiangkou Reservoir (storage: 17.5 km^3) on the upper Hanjiang River was constructed in 1968. Unfortunately, the retrieved data for the Hanjiang River started from the 1970s, rendering it impossible to compare the $p\mathrm{CO_2}$ differences between pre- and post-dam periods. Indirect evidence is that an elevated pH within the reservoir has been measured (7.95–8.33; Li et al., 2009) relative to the 1970s (7.84 ± 0.15). In the lower reach near the estuary (Fig. 3b), more pronounced net-heterotrophy and human activity could explain its high $p\mathrm{CO_2}$. Settling down of particulate organic matter coupled with nutrient-rich water plume from offshore can accelerate CO_2 production. Chen et al. (2008) concluded that aerobic respiration of heterotrophic ecosystems was the primary determinant of the high $p\mathrm{CO_2}$ in the inner Yangtze estuary. Moreover, the lower Yangtze River watershed was highly populated. Inputs of acids from agricultural fertilizer, sewage, and acid deposition have also decreased pH and shifted the carbonate system towards CO_2 (Duan et al., 2007; Chen et al., 2002), generating high $p\mathrm{CO_2}$ values regardless of its relatively low alkalinity.

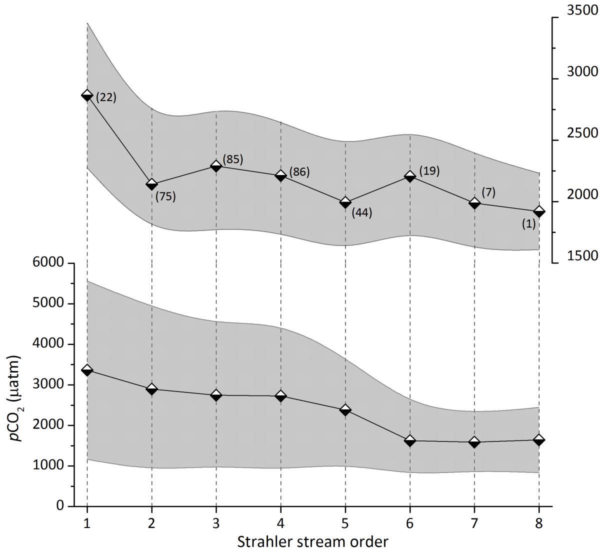

Figure 8. Decreasing alkalinity (top) and $p\mathrm{CO_2}$ (bottom) with increasing Strahler stream order. The grey shade denotes standard deviation and the numbers in parentheses represent the number of stations aggregated for each stream order.

4.3 Geomorphological controls on alkalinity and $p\mathrm{CO_2}$

To illustrate the geomorphological controls, the 339 stations used were aggregated by stream order based on their spatial positions. Both alkalinity and $p\mathrm{CO_2}$ showed a decreasing trend from the smallest headwater streams through tributaries to the Yangtze mainstem (Fig. 8). The average decrease of alkalinity and $p\mathrm{CO_2}$ were 94 μeq L^{-1} and 266 μatm, respectively. Higher alkalinity and $p\mathrm{CO_2}$ in the headwater streams reveal the significance of direct terrestrial inputs of organic carbon and dissolved CO_2 in controlling riverine carbon cycle. Over the study period, the Yangtze River watershed suffered severe soil erosion, averaging 2167 t km^{-2} yr^{-1} (Z. Y. Wang et al., 2007). Huge amounts of carbon were transported into the river system via erosion (Wu et al., 2007). Decomposition of the terrestrial-origin organic carbon has resulted in the CO_2 excess in the headwater streams (Li et al., 2012).

The decreasing $p\mathrm{CO_2}$ with increasing stream order imply continued CO_2 evasion along the river continuum and reduced supply of fresh CO_2. Except for the three lakes connected to the mainstem (Fig. 1a), the Yangtze River network is largely confined to its channel. Without large floodplains supplying labile organic matter to sustain high $p\mathrm{CO_2}$ as in the Amazon River (Mayorga et al., 2005), its $p\mathrm{CO_2}$ decreased progressively from the headwaters towards the mainstem channel. In addition, it is interesting to note that the $p\mathrm{CO_2}$ in the highest three orders was equivalent ($\sim$ 1800 μatm; Fig. 8). Instead of continuous decline, the stable $p\mathrm{CO_2}$ suggests a balance between CO_2 evasion and supply of fresh CO_2 from upstream catchments or aquatic respiration. Contrary to the headwater streams with close contact with terrestrial ecosystems, the downstream large streams and rivers are far away from rapid fresh CO_2 input. Moreover, these large streams and rivers are generally characterized by comparatively low gas transfer velocities due to weakened turbulence and mixing with benthic substrates (Butman and Raymond, 2011; Borges et al., 2015), which can effectively inhibit CO_2 degassing and therefore maintain the balance. An example is the Yangtze estuary, which presents considerably low CO_2 evasion fluxes of 16–34 $\mathrm{mol\,m^{-2}\,yr^{-1}}$, despite its significantly higher riverine $p\mathrm{CO_2}$ than the overlying atmosphere (Zhai et al., 2007).

It is important to note, however, that the delineated eight stream orders may not necessarily represent the actual stream network. Limited by spatial resolution, the smallest headwater streams might have been missed from the identified river network. In addition, these headwater streams are also generally absent of sampling stations. With much closer biogeochemical interactions with land ecosystems, these missed headwater streams tend to have higher $p\mathrm{CO_2}$ (Benstead and Leigh, 2012; Aufdenkampe et al., 2011; Butman and Raymond, 2011). Thus, the actual $p\mathrm{CO_2}$ gradient along the stream order may be sharper if a higher $p\mathrm{CO_2}$ in the headwater streams is included.

4.4 Implications for riverine CO_2 evasion

As mentioned earlier, riverine carbon transport has been a significant component of the carbon cycle. Quantifying riverine carbon export is essential to better evaluate global carbon budget and elucidate the magnitude of carbon exchange between different pools. For the estimation of CO_2 evasion, riverine $p\mathrm{CO_2}$ denotes CO_2 concentration gradient across the water–air interface and thus the potential of CO_2 exchange. Prior studies indicate that elevated riverine $p\mathrm{CO_2}$ can enhance CO_2 evasion owing to a steeper concentration gradient and a greater CO_2 availability for degassing (Long et al., 2015; Billett and Moore, 2008). When assessing global-scale CO_2 evasion, however, the spatial distribution of $p\mathrm{CO_2}$ is heavily skewed towards North America, Europe, and Australia (e.g., Lauerwald et al., 2015; Raymond et al., 2013), while data for Asian rivers are extremely lacking. This absence of an equally distributed $p\mathrm{CO_2}$ database has made it challenging to accurately estimate global CO_2 evasion. The role of Asian rivers in global carbon export explicitly demonstrates that underrepresentation of Asian rivers would cause huge biases.

Comparing the Yangtze River with other rivers shows that its $p\mathrm{CO_2}$ is higher than most world rivers (Table 4). The average $p\mathrm{CO_2}$ of 2662 µatm suggests that the Yangtze River waters are potentially a prominent carbon source for the atmosphere. Large CO_2 evasion fluxes have been reported by several small-scale studies in the upper reach and the estuary (Zhai et al., 2007; Chen et al., 2008; Li et al., 2012), as also shown in Table 4. Nonetheless, a systematic estimation of CO_2 evasion from the whole Yangtze River network, including mainstem and its tributaries of all orders, remains lacking. This has hampered the assessment of its CO_2 evasion in a wider context linking the watershed's land–atmosphere and land–ocean carbon exchanges.

Accelerated human activity is another urgent issue to be considered when investigating its riverine $p\mathrm{CO_2}$ and CO_2 evasion. Approximately 50 000 dams, including the world's largest reservoir (i.e., the Three Gorges Reservoir, TGR), have been constructed in recent decades (Xu and Milliman, 2009). Assessing the impacts of dam-triggered changes to flow regime and biogeochemical processes on $p\mathrm{CO_2}$ and CO_2 evasion is particularly important for deeper insights into its riverine carbon cycle (Table 4). For example, while the $p\mathrm{CO_2}$ at Datong station declined continuously before the TGR impoundment (Fig. 4a; F. S. Wang et al., 2007), our recent field survey shows that it has recovered from 1440 µatm in the 1980s to present 1700 µatm (see Fig. 4a). As for CO_2 degassing, recent work in the TGR indicates that its CO_2 evasion fluxes are different from natural rivers and are higher than other temperate reservoirs (Table 4; Zhao et al., 2013). Future research efforts are warranted to conduct systematic monitoring and evasion estimation. Given the Yangtze River's role in global carbon export, a comprehensive assessment of CO_2 evasion is also meaningful for global carbon budget.

5 Conclusions

By using long-term water chemistry data measured in the Yangtze River watershed during the period 1960s–1985, we calculated its $p\mathrm{CO_2}$ from pH and alkalinity. The pH in the Yangtze River waters varied from 6.5 to 9.2 and the alkalinity ranged from 415 to > 3400 $\mathrm{\mu eq\,L^{-1}}$ with high alkalinity concentrations occurring in carbonate-rich tributary catchments. Except one station in the upper reach showing a lower $p\mathrm{CO_2}$ than the atmosphere, the Yangtze River waters were supersaturated with dissolved CO_2, generally 2–20-fold the atmospheric equilibrium. Averaged over all stations, the basin-wide $p\mathrm{CO_2}$ was 2662 ± 1240 µatm. As an important parameter for CO_2 evasion estimation, its $p\mathrm{CO_2}$ was characterized by significant spatial and temporal variability, which was collectively controlled by carbon inputs from terrestrial ecosystems, hydrological regime, and rock weathering. High $p\mathrm{CO_2}$ values were observed spatially in catchments with abundant carbonate presence and seasonally in the wet season when recently fixed organic matter was flushed into the river network. Decomposition of organic matter by microbial activity in aquatic systems facilitated CO_2 production and sustained the high $p\mathrm{CO_2}$ values in wet seasons, although the alkalinity presented a significant dilution effect with water discharge. In addition, the $p\mathrm{CO_2}$ decreased with increasing stream orders from the smallest headwater streams through tributaries

Table 4. Comparison of $p\mathrm{CO_2}$ and $\mathrm{CO_2}$ evasion among world large rivers and typical reservoirs in the Yangtze River basin.

River	Country	Climate	$p\mathrm{CO_2}$ µatm	$\mathrm{CO_2}$ evasion $\mathrm{mol\,m^{-2}\,yr^{-1}}$	Reference
Yangtze network	China	Subtropical monsoon	2662 ± 1240	/	This study
Upper Yangtze	China	Subtropical monsoon	2100	57	Li et al. (2012)
Lower Yangtze	China	Subtropical monsoon	1297 ± 901	14.2−54.4	F. S. Wang et al. (2007)
Yangtze estuary	China	Subtropical monsoon	650–1440	15.5–34.2	Zhai et al. (2007)
Amazon	Brazil	Tropical	3929	162.2	Lauerwald et al. (2015)
Ottawa	Canada	Temperate	1200	14.2	Telmer and Veizer (1999)
Hudson	USA	Temperate	1125 ± 403	5.8–13.5	Raymond et al. (1997)
York estuary	USA	Temperate	1070 ± 867	6.3	Raymond et al. (2000)
Mississippi	USA	Temperate	1335 ± 130	98.5 ± 32.5	Dubois et al. (2010)
Yukon	Canada	Subarctic	582–705	11.6–21.2	Lauerwald et al. (2015)
Yellow	China	Arid and semiarid	2810 ± 1985	312.4 ± 149.2	Ran et al. (2015b)
Xijiang (Pearl)	China	Subtropical monsoon	2600	69.2–130	Yao et al. (2007)
Mekong (> 100 m wide rivers)	SE Asia	Tropical monsoon	703–1597	32–138	Alin et al. (2011)
Godavari estuary	India	Tropical monsoon	< 500–33 000	52.6	Sarma et al. (2011)
Global rivers			2400	131.2	Lauerwald et al. (2015)
Typical reservoirs in the Yangtze River basin					
Wujiang cascade reservoirs			38–3300	−3.3–32.5	Wang et al. (2011)
Three Gorges Reservoir (TGR)			/	35.1	Zhao et al. (2013)

to the mainstem channel. A higher $p\mathrm{CO_2}$ in the headwater streams illustrated the influence of direct inputs of terrestrially derived organic matter and weathering products via erosion and flushing on riverine carbon dynamics.

The substantially higher $p\mathrm{CO_2}$ than the atmosphere indicated a potential of significant $\mathrm{CO_2}$ emissions from the Yangtze River fluvial network. Quantifying the amount of $\mathrm{CO_2}$ evasion should be a top priority, upon which its biogeochemical implications for watershed-scale carbon cycle can be assessed in association with carbon burial and downstream export. Given the extensive and intensive human disturbances within the watershed since the 1990s, special attention must be paid to the resulting changes to riverine $p\mathrm{CO_2}$ and $\mathrm{CO_2}$ evasion. A comparative analysis involving $\mathrm{CO_2}$ evasion before large-scale human impacts and recent degassing estimates (e.g., Li et al., 2012; Liu et al., 2016) will be able to examine the anthropogenic perturbations of the river–atmosphere $\mathrm{CO_2}$ fluxes due to damming and land-use change. Considering the Yangtze River's relevance to global carbon export, quantifying its $\mathrm{CO_2}$ evasion is also of paramount importance for better assessments of global carbon budget.

Data availability. The data used in this study are available in the Supplement.

The Supplement related to this article is available online at doi:10.5194/bg-14-2183-2017-supplement.

Competing interests. The authors declare that they have no conflict of interest.

Acknowledgements. This work was financially supported by the University of Hong Kong (grant no. 201612159004) and the National University of Singapore (grant no. R-109-000-172-646). We gratefully thank the two anonymous reviewers for their constructive comments that greatly improved the manuscript.

Edited by: T. J. Battin
Reviewed by: two anonymous referees

References

Abril, G., Martinez, J.-M., Artigas, L. F., Moreira-Turcq, P., Benedetti, M. F., Vidal, L., Meziane, T., Kim, J.-H., Bernardes, M. C., and Savoye, N.: Amazon River carbon dioxide outgassing fuelled by wetlands, Nature, 505, 395–398, 2014.

Abril, G., Bouillon, S., Darchambeau, F., Teodoru, C. R., Marwick, T. R., Tamooh, F., Ochieng Omengo, F., Geeraert, N., Deirmendjian, L., Polsenaere, P., and Borges, A. V.: Technical Note: Large overestimation of $p\mathrm{CO_2}$ calculated from pH and alkalinity in acidic, organic-rich freshwaters, Biogeosciences, 12, 67–78, doi:10.5194/bg-12-67-2015, 2015.

Alekin, O. A., Semenov, A. D., and Skopintsev, B. A.: Handbook of Chemical Analysis of Land Waters, Gidrometeoizdat, St. Petersburg, Russia, 1973.

Alin, S. R., Rasera, M. d. F. F. L., Salimon, C. I., Richey, J. E., Holtgrieve, G. W., Krusche, A. V., and Snidvongs, A.: Physical controls on carbon dioxide transfer velocity and flux in low-gradient river systems and implications for regional carbon budgets, J. Geophys. Res., 116, G01009, doi:10.1029/2010jg001398, 2011.

American Public Health Association (APHA): Standard Methods for the Examination of Water and Wastewater, 16th edition, American Public Health Association, Washington, DC, USA, 1985.

Amiotte-Suchet, P. A., Probst, J. L., and Ludwig, W.: Worldwide distribution of continental rock lithology: Implications for the atmospheric/soil CO_2 uptake by continental weathering and alkalinity river transport to the oceans, Global Biogeochem. Cy., 17, 1038, doi:10.1029/2002gb001891, 2003.

Aufdenkampe, A. K., Mayorga, E., Raymond, P. A., Melack, J. M., Doney, S. C., Alin, S. R., Aalto, R. E., and Yoo, K.: Riverine coupling of biogeochemical cycles between land, oceans, and atmosphere, Front. Ecol. Environ., 9, 53–60, 2011.

Bao, H., Wu, Y., and Zhang, J.: Spatial and temporal variation of dissolved organic matter in the Changjiang: fluvial transport and flux estimation, J. Geophys. Res.-Biogeo., 120, 1870–1886, 2015.

Barros, N., Cole, J. J., Tranvik, L. J., Prairie, Y. T., Bastviken, D., Huszar, V. L., Del Giorgio, P., and Roland, F.: Carbon emission from hydroelectric reservoirs linked to reservoir age and latitude, Nat. Geosci., 4, 593–596, 2011.

Battin, T. J., Luyssaert, S., Kaplan, L. A., Aufdenkampe, A. K., Richter, A., and Tranvik, L. J.: The boundless carbon cycle, Nat. Geosci., 2, 598–600, 2009.

Benstead, J. P. and Leigh, D. S.: An expanded role for river networks, Nat. Geosci., 5, 678–679, 2012.

Billett, M. and Moore, T.: Supersaturation and evasion of CO_2 and CH_4 in surface waters at Mer Bleue peatland, Canada, Hydrol. Process., 22, 2044–2054, 2008.

Borges, A. V., Darchambeau, F., Teodoru, C. R., Marwick, T. R., Tamooh, F., Geeraert, N., Omengo, F. O., Guérin, F., Lambert, T., and Morana, C.: Globally significant greenhouse-gas emissions from African inland waters, Nat. Geosci., 8, 637–642, 2015.

Butman, D. and Raymond, P. A.: Significant efflux of carbon dioxide from streams and rivers in the United States, Nat. Geosci., 4, 839–842, 2011.

Cauwet, G. and Mackenzie, F. T.: Carbon inputs and distribution in estuaries of turbid rivers: the Yang Tze and Yellow rivers (China), Mar. Chem., 43, 235–246, 1993.

Chen, C.-T. A., Zhai, W., and Dai, M.: Riverine input and air-sea CO_2 exchanges near the Changjiang (Yangtze River) Estuary: status quo and implication on possible future changes in metabolic status, Cont. Shelf Res., 28, 1476–1482, 2008.

Chen, J., Wang, F. Y., Xia, X. H., and Zhang, L. T.: Major element chemistry of the Changjiang (Yangtze River), Chem. Geol., 187, 231–255, 2002.

Chetelat, B., Liu, C. Q., Zhao, Z., Wang, Q., Li, S., Li, J., and Wang, B.: Geochemistry of the dissolved load of the Changjiang Basin rivers: anthropogenic impacts and chemical weathering, Geochim. Cosmochim. Ac., 72, 4254–4277, 2008.

Cole, J. J., Prairie, Y. T., Caraco, N. F., McDowell, W. H., Tranvik, L. J., Striegl, R. G., Duarte, C. M., Kortelainen, P., Downing, J. A., Middelburg, J. J., and Melack, J.: Plumbing the global carbon cycle: Integrating inland waters into the terrestrial carbon budget, Ecosystems, 10, 171–184, 2007.

Duan, S., Xu, F., and Wang, L.-J.: Long-term changes in nutrient concentrations of the Changjiang River and principal tributaries, Biogeochemistry, 85, 215–234, 2007.

Dubois, K. D., Lee, D., and Veizer, J.: Isotopic constraints on alkalinity, dissolved organic carbon, and atmospheric carbon dioxide fluxes in the Mississippi River, J. Geophys. Res.-Biogeo., 115, G02018, doi:10.1029/2009JG001102, 2010.

Gan, W. B., Chen, H. M., and Hart, Y. F.: Carbon transport by the Yangtze (at Nanjing) and Huanghe (at Jinan) Rivers, People's Republic of China, in: Transport of Carbon and Minerals in Major World Rivers, Part 2, edited by: Degens, E. T., Kempe, S., and Soliman, H., Mitt. Geol. Paläontol. Inst. Univ. Hamburg, SCOPE/UNEP Sonderbd., 459–470, 1983.

Goudie, A. S. and Viles, H. A.: Weathering and the global carbon cycle: Geomorphological perspectives, Earth-Sci. Rev., 113, 59–71, 2012.

Hope, D., Billett, M., and Cresser, M.: A review of the export of carbon in river water: fluxes and processes, Environ. Pollut., 84, 301–324, 1994.

Humborg, C., Mörth, C., Sundbom, M., Borg, H., Blenckner, T., Giesler, R., and Ittekkot, V.: CO_2 supersaturation along the aquatic conduit in Swedish watersheds as constrained by terrestrial respiration, aquatic respiration and weathering, Glob. Change Biol., 16, 1966–1978, 2010.

Hunt, C. W., Salisbury, J. E., and Vandemark, D.: Contribution of non-carbonate anions to total alkalinity and overestimation of $p\mathrm{CO}_2$ in New England and New Brunswick rivers, Biogeosciences, 8, 3069–3076, doi:10.5194/bg-8-3069-2011, 2011.

Ittekkot, V.: Global trends in the nature of organic matter in river suspensions, Nature, 332, 436–438, 1988.

Kemenes, A., Forsberg, B. R., and Melack, J. M.: CO_2 emissions from a tropical hydroelectric reservoir (Balbina, Brazil), J. Geophys. Res., 116, G03004, doi:10.1029/2010JG001465, 2011.

Laruelle, G. G., Dürr, H. H., Lauerwald, R., Hartmann, J., Slomp, C. P., Goossens, N., and Regnier, P. A. G.: Global multi-scale segmentation of continental and coastal waters from the watersheds to the continental margins, Hydrol. Earth Syst. Sci., 17, 2029–2051, doi:10.5194/hess-17-2029-2013, 2013.

Lauerwald, R., Hartmann, J., Moosdorf, N., Kempe, S., and Raymond, P. A.: What controls the spatial patterns of the riverine carbonate system? – A case study for North America, Chem. Geol., 337–338, 114–127, 2013.

Lauerwald, R., Laruelle, G. G., Hartmann, J., Ciais, P., and Regnier, P. A.: Spatial patterns in CO_2 evasion from the global river network, Global Biogeochem. Cy., 29, 534–554, 2015.

Lewis, E. and Wallace, D. W. R.: Program developed for CO_2 system calculations. ORNL/CDIAC-105, Carbon dioxide Information Analysis Center, Oak Ridge National Laboratory, Oak Ridge, TN, USA, 1998.

Li, S., Cheng, X., Xu, Z., Han, H., and Zhang, Q.: Spatial and temporal patterns of the water quality in the Danjiangkou Reservoir, China, Hydrolog. Sci. J., 54, 124–134, 2009.

Li, S., Lu, X. X., He, M., Zhou, Y., Li, L., and Ziegler, A. D.: Daily CO_2 partial pressure and CO_2 outgassing in the upper Yangtze River basin: A case study of the Longchuan River, China, J. Hydrol., 466–467, 141–150, 2012.

Li, S.-L., Liu, C.-Q., Li, J., Lang, Y.-C., Ding, H., and Li, L.: Geochemistry of dissolved inorganic carbon and carbonate weathering in a small typical karstic catchment of Southwest China:

Isotopic and chemical constraints, Chem. Geol., 277, 301–309, 2010.

Li, X.-D., Liu, C.-Q., Harue, M., Li, S.-L., and Liu, X.-L.: The use of environmental isotopic (C, Sr, S) and hydrochemical tracers to characterize anthropogenic effects on karst groundwater quality: A case study of the Shuicheng Basin, SW China, Appl. Geochem., 25, 1924–1936, 2010.

Liu, S., Lu, X. X., Xia, X., Zhang, S., Ran, L., Yang, X., and Liu, T.: Dynamic biogeochemical controls on river $p\mathrm{CO}_2$ and recent changes under aggravating river impoundment: an example of the subtropical Yangtze River, Global Biogeochem. Cy., 30, 880–897, 2016.

Long, H., Vihermaa, L., Waldron, S., Hoey, T., Quemin, S., and Newton, J.: Hydraulics are a first-order control on CO_2 efflux from fluvial systems, J. Geophys. Res.-Biogeo., 120, 1912–1922, 2015.

Lynch, J. K., Beatty, C. M., Seidel, M. P., Jungst, L. J., and DeGrandpre, M. D.: Controls of riverine CO_2 over an annual cycle determined using direct, high temporal resolution pCO_2 measurements, J. Geophys. Res., 115, G03016, doi:10.1029/2009jg001132, 2010.

Marcé, R., Obrador, B., Morguí, J.-A., Riera, J. L., López, P., and Armengol, J.: Carbonate weathering as a driver of CO_2 supersaturation in lakes, Nat. Geosci., 8, 107–111, 2015.

Mayorga, E., Aufdenkampe, A. K., Masiello, C. A., Krusche, A. V., Hedges, J. I., Quay, P. D., Richey, J. E., and Brown, T. A.: Young organic matter as a source of carbon dioxide outgassing from Amazonian rivers, Nature, 436, 538–541, 2005.

Milliman, J. D., Qinchun, X., and Zuosheng, Y.: Transfer of particulate organic carbon and nitrogen from the Yangtze River to the ocean, Am. J. Sci., 284, 824–834, 1984.

Ran, L., Lu, X. X., Richey, J. E., Sun, H., Han, J., Yu, R., Liao, S., and Yi, Q.: Long-term spatial and temporal variation of CO_2 partial pressure in the Yellow River, China, Biogeosciences, 12, 921–932, doi:10.5194/bg-12-921-2015, 2015a.

Ran, L., Lu, X. X., Yang, H., Li, L., Yu, R., Sun, H., and Han, J.: CO_2 outgassing from the Yellow River network and its implications for riverine carbon cycle, J. Geophys. Res.-Biogeo., 120, 1334–1347, 2015b.

Raymond, P. A. and Cole, J. J.: Increase in the export of alkalinity from North America's largest river, Science, 301, 88–91, 2003.

Raymond, P. A., Caraco, N. F., and Cole, J. J.: Carbon dioxide concentration and atmospheric flux in the Hudson River, Estuaries, 20, 381–390, 1997.

Raymond, P. A., Bauer, J. E., and Cole, J. J.: Atmospheric CO_2 evasion, dissolved inorganic carbon production, and net heterotrophy in the York River estuary, Limnol. Oceanogr., 45, 1707–1717, 2000.

Raymond, P. A., Hartmann, J., Lauerwald, R., Sobek, S., McDonald, C., Hoover, M., Butman, D., Striegl, R., Mayorga, E., and Humborg, C.: Global carbon dioxide emissions from inland waters, Nature, 503, 355–359, 2013.

Regnier, P., Friedlingstein, P., Ciais, P., Mackenzie, F. T., Gruber, N., Janssens, I. A., Laruelle, G. G., Lauerwald, R., Luyssaert, S., and Andersson, A. J.: Anthropogenic perturbation of the carbon fluxes from land to ocean, Nat. Geosci., 6, 597–607, 2013.

Richey, J. E., Melack, J. M., Aufdenkampe, A. K., Ballester, V. M., and Hess, L. L.: Outgassing from Amazonian rivers and wetlands as a large tropical source of atmospheric CO_2, Nature, 416, 617–620, 2002.

Sarma, V. V. S. S., Kumar, N. A., Prasad, V. R., Venkataramana, V., Appalanaidu, S., Sridevi, B., Kumar, B. S. K., Bharati, M. D., Subbaiah, C. V., Acharyya, T., Rao, G. D., Viswanadham, R., Gawade, L., Manjary, D. T., Kumar, P. P., Rajeev, K., Reddy, N. P. C., Sarma, V. V., Kumar, M. D., Sadhuram, Y., and Murty, T. V. R.: High CO_2 emissions from the tropical Godavari estuary (India) associated with monsoon river discharges, Geophys. Res. Lett., 38, L08601, doi:10.1029/2011gl046928, 2011.

Schlünz, B. and Schneider, R. R.: Transport of terrestrial organic carbon to the oceans by rivers: re-estimating flux- and burial rates, Int. J. Earth Sci., 88, 599–606, 2000.

Syvitski, J. P. M., Vorosmarty, C. J., Kettner, A. J., and Green, P.: Impact of humans on the flux of terrestrial sediment to the global coastal ocean, Science, 308, 376–380, 2005.

Telmer, K. and Veizer, J.: Carbon fluxes, pCO_2 and substrate weathering in a large northern river basin, Canada: carbon isotope perspectives, Chem. Geol., 159, 61–86, 1999.

Teodoru, C. R., Nyoni, F. C., Borges, A. V., Darchambeau, F., Nyambe, I., and Bouillon, S.: Dynamics of greenhouse gases (CO_2, CH_4, N_2O) along the Zambezi River and major tributaries, and their importance in the riverine carbon budget, Biogeosciences, 12, 2431–2453, doi:10.5194/bg-12-2431-2015, 2015.

Wallin, M. B., Grabs, T., Buffam, I., Laudon, H., Ågren, A., Öquist, M. G., and Bishop, K.: Evasion of CO_2 from streams–The dominant component of the carbon export through the aquatic conduit in a boreal landscape, Glob. Change Biol., 19, 785–797, 2013.

Wallin, M. B., Löfgren, S., Erlandsson, M., and Bishop, K.: Representative regional sampling of carbon dioxide and methane concentrations in hemiboreal headwater streams reveal underestimates in less systematic approaches, Global Biogeochem. Cy., 28, 465–479, 2014.

Wang, F. S., Wang, Y. C., Zhang, J., Xu, H., and Wei, X. G.: Human impact on the historical change of CO_2 degassing flux in River Changjiang, Geochem. T., 8, 1–10, doi:10.1186/1467-4866-8-7, 2007.

Wang, F. S., Wang, B. L., Liu, C. Q., Wang, Y. C., Guan, J., Liu, X. L., and Yu, Y. X.: Carbon dioxide emission from surface water in cascade reservoirs-river system on the Maotiao River, southwest of China, Atmos. Environ., 45, 3827–3834, 2011.

Wang, X., Ma, H., Li, R., Song, Z., and Wu, J.: Seasonal fluxes and source variation of organic carbon transported by two major Chinese Rivers: The Yellow River and Changjiang (Yangtze) River, Global Biogeochem. Cy., 26, GB2025, doi:10.1029/2011gb004130, 2012.

Wang, Z. Y., Li, Y., and He, Y.: Sediment budget of the Yangtze River, Water Resour. Res., 43, W04401, doi:10.1029/2006WR005012, 2007.

Wanninkhof, R., Park, G.-H., Takahashi, T., Sweeney, C., Feely, R., Nojiri, Y., Gruber, N., Doney, S. C., McKinley, G. A., Lenton, A., Le Quéré, C., Heinze, C., Schwinger, J., Graven, H., and Khatiwala, S.: Global ocean carbon uptake: magnitude, variability and trends, Biogeosciences, 10, 1983–2000, doi:10.5194/bg-10-1983-2013, 2013.

Weyhenmeyer, G. A., Kosten, S., Wallin, M. B., Tranvik, L. J., Jeppesen, E., and Roland, F.: Significant fraction of CO_2 emissions from boreal lakes derived from hydrologic inorganic carbon inputs, Nat. Geosci., 8, 933–936, 2015.

Wu, Y., Zhang, J., Liu, S. M., Zhang, Z. F., Yao, Q. Z., Hong, G. H., and Cooper, L.: Sources and distribution of carbon within the Yangtze River system, Estuar. Coast. Shelf S., 71, 13–25, 2007.

Xu, K. and Milliman, J. D.: Seasonal variations of sediment discharge from the Yangtze River before and after impoundment of the Three Gorges Dam, Geomorphology, 104, 276–283, 2009.

Yang, S., Zhao, Q., and Belkin, I. M.: Temporal variation in the sediment load of the Yangtze river and the influences of human activities, J. Hydrol., 263, 56–71, 2002.

Yao, G. R., Gao, Q. Z., Wang, Z. G., Huang, X. K., He, T., Zhang, Y. L., Jiao, S. L., and Ding, J.: Dynamics of CO_2 partial pressure and CO_2 outgassing in the lower reaches of the Xijiang River, a subtropical monsoon river in China, Sci. Total Environ., 376, 255–266, 2007.

Zhai, W. D., Dai, M. H., and Guo, X. G.: Carbonate system and CO_2 degassing fluxes in the inner estuary of Changjiang (Yangtze) River, China, Mar. Chem., 107, 342–356, 2007.

Zhang, L., Xue, M., Wang, M., Cai, W.-J., Wang, L., and Yu, Z.: The spatiotemporal distribution of dissolved inorganic and organic carbon in the main stem of the Changjiang (Yangtze) River and the effect of the Three Gorges Reservoir, J. Geophys. Res.-Biogeo., 119, 741–757, 2014.

Zhao, Y., Wu, B. F., and Zeng, Y.: Spatial and temporal patterns of greenhouse gas emissions from Three Gorges Reservoir of China, Biogeosciences, 10, 1219–1230, doi:10.5194/bg-10-1219-2013, 2013.